JPn Neuroscience

The Journal of Physiology

J Physiol 590.16 (2012) pp 3787–3805

Two $GABA_A$ responses with distinct kinetics in a sound localization circuit

Zheng-Quan Tang and Yong Lu

Department of Anatomy and Neurobiology, College of Medicine, Northeast Ohio Medical University, Rootstown, OH 44272, USA

Key points

- It is known that synaptic inhibition plays important roles in auditory binaural neurons involved in sound localization.
- Here, we show that GABAergic inhibition exhibits characteristic frequency (CF)-dependent kinetics in auditory binaural neurons.
- We further show that differential profiles of asynchronous release and spillover of GABA account for the distinct kinetics.
- GABAergic inhibition regulates neuronal excitability in a CF-dependent manner.
- The results suggest that GABAergic inhibition may exert a dynamic modulation of sound localization processing in a CF-dependent manner.

Abstract The temporal characteristics and functional diversity of GABAergic inhibition are determined by the spatiotemporal neurotransmitter profile, intrinsic properties of $GABA_A$ receptors, and other factors. Here, we report two distinct $GABA_A$ responses and the underlying mechanisms in neurons of the chicken nucleus laminaris (NL), the first encoder of interaural time difference for sound localization in birds. The time course of the postsynaptic $GABA_A$ currents in NL neurons, recorded with whole-cell voltage clamp, differed between different characteristic frequency (CF) regions. Compared to low-CF (LF) neurons, middle/high-CF (MF/HF) neurons had significantly slower IPSCs, with a 2.6-fold difference in the decay time constants of spontaneous IPSCs and a 5.3-fold difference in the decay of IPSCs elicited by single-pulse stimulus. Such differences were especially dramatic when IPSCs were elicited by train stimulations at physiologically relevant frequencies, and at high stimulus intensities. To account for these distinct $GABA_A$ responses, we showed that MF/HF neurons exhibited more prominent asynchronous release of GABA. Supporting this observation, replacement of extracellular Ca^{2+} with Sr^{2+} increased the decay of IPSCs in LF neurons, and EGTA-AM reduced the decay of IPSCs in MF/HF neurons. Furthermore, pharmacological evidence suggests that GABA spillover plays a greater role in prolonging the IPSCs of MF/HF neurons. Consequently, under whole-cell current clamp, synaptically released GABA produced short- and long-lasting suppression of the neuronal excitability of LF and MF/HF neurons, respectively. Taken together, these results suggest that the GABAergic inputs to NL neurons may exert a dynamic modulation of interaural time difference (ITD) coding in a CF-dependent manner.

(Received 9 January 2012; accepted after revision 16 May 2012; first published online 21 May 2012)

Corresponding author Z-Q. Tang or Y. Lu: Department of Anatomy and Neurobiology, College of Medicine, Northeast Ohio Medical University, Rootstown, OH 44272, USA. Email: ztang@neomed.edu or ylu@neomed.edu

Abbreviations CF, characteristic frequency; GABA, γ-aminobutyric acid; $GABA_AR$, γ-aminobutyric acid A receptor; IPSC, inhibitory postsynaptic current; IPSP, inhibitory postsynaptic potential; ITD, interaural time difference; NL, nucleus laminaris; SON, superior olivary nucleus; VGCC, voltage-gated calcium channel.

DOI: 10.1113/jphysiol.2012.230136

Introduction

Based on the time course of the postsynaptic responses, GABAergic inhibition mediated by ionotropic $GABA_A$ receptors ($GABA_A$Rs) is classified into two basic types, phasic and tonic inhibition. Phasic inhibition results from the activation of low-affinity synaptic $GABA_A$Rs by transient GABA release, whereas tonic inhibition is mediated by persistent activation of extrasynaptic $GABA_A$Rs by ambient GABA (Farrant & Nusser, 2005). Phasic inhibition is further divided into a classically rapid inhibition and a slow inhibition (Capogna & Pearce, 2011), with the decay of IPSCs of the latter lasting tens to hundreds of milliseconds. Some neurons may receive both forms of inhibition at different cellular locations (Pearce, 1993). Several factors, including the spatiotemporal transmitter profile and the biophysical properties of postsynaptic receptors, have been suggested to underlie the slow inhibition (Capogna & Pearce, 2011).

In the avian auditory brainstem, the nucleus laminaris (NL), an analogue of the mammalian medial superior olive, is essential in processing information for sound localization in azimuth. NL neurons act as coincidence detectors for converging binaural excitatory inputs, encoding separately at each characteristic frequency (CF) the extremely small interaural time difference (ITD, μs range) in order for the animal to determine the position of a sound source (Köppl & Carr, 2008; Kandler *et al.* 2009; Seidl *et al.* 2010). While bilaterally segregated excitatory inputs to NL are essential for ITD coding, the inhibitory inputs play a critical role in modulating ITD processing (Grothe, 2003; Nishino *et al.* 2008; Burger *et al.* 2011). There are abundant GABAergic terminals impinging on the soma and dendrites of NL neurons (Carr *et al.* 1989; Code *et al.* 1989; Tabor *et al.* 2011). The primary source of these GABAergic terminals is the ipsilateral superior olivary nucleus (SON) (Lachica *et al.* 1994; Yang *et al.* 1999; Burger *et al.* 2005; Tabor *et al.* 2011), with additional contributions from local GABAergic neurons sparsely distributed in and around NL (Code *et al.* 1989).

Physiological studies suggest that NL neurons receive multiple types of $GABA_A$R-mediated inhibition. A background tonic inhibition mediated by extrasynaptic δ-containing $GABA_A$Rs expresses predominantly in middle/high-CF (MF/HF), but not in low-CF (LF) neurons (Tang *et al.* 2011), indicating that the tonic GABAergic inhibition is CF dependent, as are other physiological properties of NL neurons such as voltage-gated Na^+ and K^+ channels (Kuba *et al.* 2005, 2006), hyperpolarization-activated cation channels (Yamada *et al.* 2005), and glutamatergic responses (Kuba *et al.* 2005; Sanchez *et al.* 2010; Slee *et al.* 2010). Kuo *et al.* (2009) recently reported a classically rapid GABAergic inhibition, whereas Funabiki *et al.* (1998) and Yang *et al.* (1999) provided evidence for long-lasting synaptic inhibition in NL neurons. The reasons for this discrepancy are unclear. We hypothesized that the phasic inhibition in NL neurons exhibited CF-dependent kinetics differences. To test this hypothesis and more importantly to reveal the underlying mechanisms, we characterized the temporal properties of GABAergic transmission in NL neurons in different CF regions, analysed the profiles of asynchronous release and spillover of GABA, and examined the regulation of neuronal excitability by GABAergic inhibition with different kinetics.

Methods

Ethical approval

The experimental procedures have been approved by the Institutional Animal Care and Use Committee (IACUC) at Northeast Ohio Medical University, and are in accordance with NIH policies on animal use.

Slice preparation and whole-cell recordings

Brainstem slices (250–300 μm thick) were prepared from chick embryos (E17–21) and early hatchings (P3) of both sexes, as described previously (Tang *et al.* 2009). Briefly, the ice-cold artificial cerebrospinal fluid (ACSF) used for dissecting and slicing the brain tissue contained (in mM): 250 glycerol, 3 KCl, 1.2 KH_2PO_4, 20 $NaHCO_3$, 3 Hepes, 1.2 $CaCl_2$, 5 $MgCl_2$, and 10 dextrose, pH 7.4 when gassed with 95% O_2 and 5% CO_2. Slices were incubated at 34–36°C for ~1 h in normal ACSF containing (in mM): 130 NaCl, 26 $NaHCO_3$, 3 KCl, 3 $CaCl_2$, 1 $MgCl_2$, 1.25 NaH_2PO_4 and 10 dextrose (pH 7.4).

The NL was divided into three CF regions (low: 0.4–1.0 kHz; middle: 1.0–2.5 kHz; and high CF: 2.5–3.3 kHz) based on the coding frequencies of neurons along the tonotopic axis (Fig. 1*A*–*B*) (Rubel & Parks, 1975; Kuba *et al.* 2005). Specifically, about five coronal brain slices (defined as slices 1–5 from rostral to caudal) containing NL were obtained from each animal. The NL in each slice was roughly divided into one to three sectors along the medial-to-lateral axis, and the CF regions were determined as previously described (Kuba *et al.* 2005). In general, the cell bodies of MF/HF neurons form a single-layer structure in the same plane of focus, whereas the cell bodies of LF neurons form multiple layers. Similar to our previous study (Tang *et al.* 2011), the neuronal properties of middle and high CF neurons we examined in this study were not significantly different, and hence we report the data for two populations of NL neurons, LF and MF/HF neurons. Voltage- and current-clamp experiments were performed with an AxoPatch 200B and an AxoClamp 2B amplifier, respectively (Molecular Devices, Union City, CA, USA). Recordings were performed in the same

ACSF as the incubation at $35 \pm 1^{\circ}$C. The electrodes had resistances between 3 and 7 MΩ when filled with a solution containing (in mM): 105 potassium gluconate, 35 KCl, 5 EGTA, 10 Hepes, 1 $MgCl_2$, 4 ATP-Mg, and 0.3 GTP-Na, with pH of 7.2 (adjusted with KOH). The Cl^- concentration (37 mM) in the internal solution was chosen to approximate the physiological Cl^- concentration in NL neurons measured with gramicidin perforated-patch recordings (Tang *et al.* 2009). The liquid junction potential was 10 mV, and data were corrected accordingly. Data were low-pass filtered at 3–10 kHz, and digitized with a Data Acquisition Interface ITC-18 (Instrutech, Great Neck, NY, USA) at 20 kHz.

Synaptic stimulation and recordings of synaptic responses

Extracellular stimulation was performed using concentric bipolar electrodes with a tip core diameter of 127 μm (World Precision Instruments, Sarasota, FL, USA). To activate the GABAergic pathway, the stimulating electrode was placed lateral to the NL using a Micromanipulator NMN-25 (Narishige, Japan). Square electric pulses of 200 μs duration were delivered through a stimulator A320RC (World Precision Instruments). IPSCs were recorded in the presence of ionotropic glutamate receptor antagonists (50 μM DNQX and 50 μM APV for AMPARs and NMDARs, respectively) and $GABA_B$ receptor blocker (10 μM CGP52432). The IPSCs were blocked by SR95531 (10 μM), a selective antagonist for $GABA_A$Rs. To compare the temporal properties of IPSCs obtained from NL neurons at different CF regions, optimal stimulus parameters were selected for each cell to give reliable post-synaptic responses close to maximal amplitude, unless otherwise indicated. For some neurons, we obtained input–output functions by recording IPSCs in response to systematically increasing stimulus intensities. When we compared the IPSCs obtained at high intensity to those obtained at low intensity in a given neuron, the high intensity was defined as the stimulus intensity that elicited responses close to maximal amplitude, and the low intensity was defined as the stimulus intensity that elicited about 25% of the maximal response.

All chemicals and drugs were obtained from Sigma (St Louis, MO, USA) except for 3-[[(3,4-dichlorophenyl) methyl]amino]propyl] diethoxymethyl)phosphinic acid (CGP52432), 1,2,5,6-tetrahydro-1-[2-[[(diphenylmethyl ene)amino]oxy]ethyl]-3-pyridinecarboxylic acid hydrochloride (NNC711), 6-imino-3-(4-methoxyphenyl)-1(6*H*) -pyridazinebutanoic acid (SR95531), and 1,2,5,6-tetrahydropyridin-4-yl)methylphosphinic acid (TPMPA), which were obtained from Tocris (Ellisville, MO, USA), and EGTA-AM, which was purchased from Invitrogen (Carlsbad, CA, USA).

Data analysis

Asynchronous release events occurring after electrical stimulations were examined and counted with visual inspection. Spontaneous IPSCs (sIPSCs) were detected by a template using a function for product of exponentials, $f(t) = [1 - \exp(-t/\text{rise time})] \times \exp(-t/\text{decay } \tau)$, in which t is time and τ is the time constant, as described previously (Tang *et al.* 2011). The decay time of the last IPSCs were fitted by single or double exponential functions. The best fit was selected by comparing the sum of squared errors between fits with single and double components. The weighted decay time constant was calculated as $\tau = (A_{\text{fast}}\tau_{\text{fast}} + A_{\text{slow}}\tau_{\text{slow}})/(A_{\text{fast}} + A_{\text{slow}})$, where A_{fast} and A_{slow} represent the amplitude, and τ_{fast} and τ_{slow} represent the time constants of the fast and slow components of the IPSC, respectively. Half-width was defined as the duration of the IPSCs measured at 50% maximum amplitude.

Graphs were made in Igor (Wavemetrics, Lake Oswego, OR, USA). Means and standard errors of the mean (SEM) are reported. Statistical differences were determined by paired or unpaired t tests, unless indicated otherwise.

Results

MF/HF NL neurons have slower IPSC kinetics compared to LF neurons

The temporal properties of both spontaneous IPSCs (sIPSCs) and evoked IPSCs were distinct between the LF and MF/HF regions (Fig. 1*C–H*). The sIPSCs in MF/HF neurons showed significantly slower decay time constants (LF: 6.9 ± 0.4 ms, $n = 27$; MF/HF: 17.6 ± 0.7 ms, $n = 49$, $P < 0.001$), while the rise times of the sIPSCs were similar (LF: 1.1 ± 0.1 ms, $n = 27$; MF/HF: 1.2 ± 0.1 ms, $n = 49$, $P > 0.05$) (Fig. 1*C–E*; Table 1). Consistent with our previous study (Tang *et al.* 2011), MF/HF neurons showed higher frequency and amplitude of sIPSCs than LF neurons (Fig. 1*E*), suggesting higher release probability and quantal size in MF/HF neurons. The sIPSCs recorded *in vitro* in our hands may represent miniature IPSCs (mIPSCs), because the amplitude histograms of sIPSCs of both LF and MF/HF neurons were unimodal and approximately normally distributed, and the mIPSCs recorded in the presence of tetrodotoxin (TTX, 1 μM) showed similar amplitude distributions (Fig. 1*F*). Furthermore, we found a significant difference in the mean amplitude of mIPSCs between LF and MF/HF neurons (Fig. 1*G*; LF: -37.5 ± 5.1 pA, $n = 5$; MF/HF: -62.7 ± 6.6 pA, $n = 5$, $P < 0.05$). Single-pulse stimulation of the GABAergic pathway evoked IPSCs with slow decay kinetics in MF/HF neurons, whereas IPSCs of similar amplitude recorded from LF neurons were significantly faster (LF: 10.4 ± 0.6 ms, $n = 21$; MF/HF:

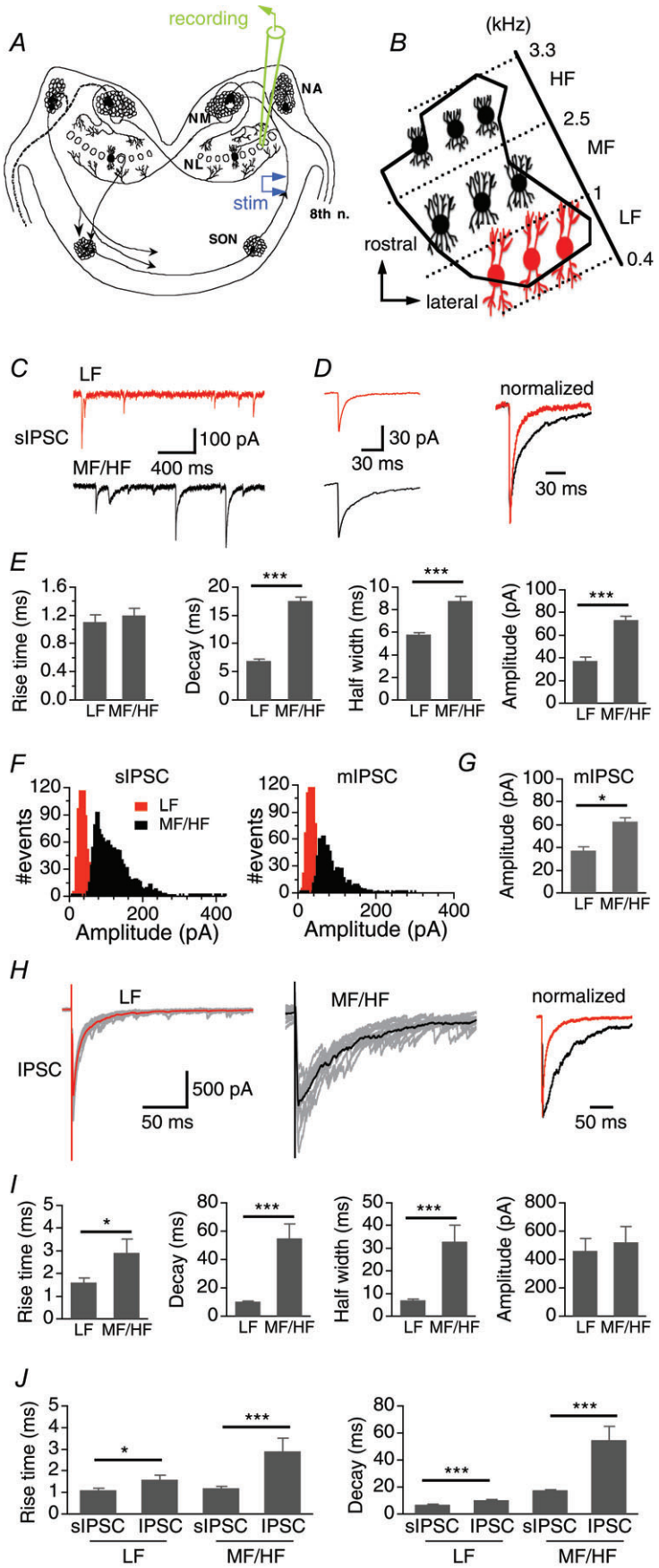

Figure 1. MF/HF NL neurons have slower IPSC kinetics compared to LF neurons
A and *B*, schematic diagram of the avian auditory brainstem. NA, nucleus angularis; NM, nucleus magnocellularis; SON, superior olivary nucleus; 8th n, cranial nerve VIII. The NL was divided into three regions according to the neurons' characteristic frequency (CF) (adapted from Rubel & Parks, 1975). LF, MF, and HF: low, middle and high CF, respectively. *C*, representative sIPSCs from a LF neuron (top panel, red) and a MF/HF neuron (lower panel, black). *D*, left, average sIPSCs. Right, average sIPSCs normalized to the peak. *E*, summary of rise time, weighted decay time constant, half-width, and amplitude of sIPSCs in LF ($n = 27$) and MF/HF neurons ($n = 49$). No significant difference was detected in rise time, whereas the decay, half-width, and the amplitude of sIPSCs of MF/HF neurons were significantly larger than those of LF neurons. *F*, representative sIPSC amplitude histograms (bin width of 5 pA) of both a LF and a MF/HF neuron showed unimodal and normal distributions. Miniature IPSCs (mIPSCs) recorded in the presence of TTX showed similar amplitude distributions. *G*, the amplitude of mIPSCs of LF neurons ($n = 5$) was significantly smaller than that of MF/HF neurons ($n = 5$). *H*, left and middle, superimposed individual IPSCs (grey) in response to single-pulse stimulations, with the average IPSCs highlighted (thick red and black traces). The IPSC amplitude was close to that of the maximal responses. Right, average IPSCs normalized to the peak. *I*, summary of rise time, weighted decay time constant, half-width, and amplitude of IPSCs in LF ($n = 21$) and MF/HF neurons ($n = 21$). IPSCs of MF/HF neurons had slower rise time, decay, and hence broader width compared to those of LF neurons. *J*, the kinetics of IPSCs elicited by single-pulse stimulations was slower than that of sIPSCs, regardless of the CF region. In this and subsequent figures, bars represent means ± SEM; $^{*}P < 0.05$, $^{**}P < 0.01$, and $^{***}P < 0.001$ (*t* test, unless indicated otherwise). Cells were held at −60 mV for voltage-clamp experiments.

Table 1. Decay time constants of IPSCs of NL neurons under different stimulus conditions

	Decay time constant (ms)	
Stimulus condition	LF (*n*)	MF/HF (*n*)
Miniature IPSC	7.2 ± 0.8(5)	16.1 ± 1.5(5)**
Spontaneous IPSC	6.9 ± 0.4(27)	17.6 ± 0.7(49)***
Single-pulse IPSC	10.4 ± 0.6(21)	54.8 ± 10.3(21)***
Train stimulations (same intensity)		
1 Hz	11.5 ± 0.9(11)	81.4 ± 22.3(8)**
5 Hz	13.2 ± 1.8	121.7 ± 26.0***
10 Hz	14.2 ± 1.7	203.6 ± 45.0***
50 Hz	33.2 ± 4.8	264.8 ± 46.5***
100 Hz	60.5 ± 6.2	327.2 ± 59.4***
200 Hz	77.5 ± 6.6	293.7 ± 59.2***
Different stimulus intensity		
Single-pulse, low intensity	12.8 ± 2.7(9)	55.9 ± 10.9(14)
Single-pulse, high intensity	12.7 ± 1.0(9)	73.4 ± 12.4(14)
t test *P* value	>0.05	<0.05
100 Hz, low intensity	68.8 ± 15.5(7)	203.3 ± 18.9(15)
100 Hz, high intensity	76.5 ± 13.1(7)	355.7 ± 26.2(15)
t test *P* value	>0.05	<0.01

n: number of cells. Weighted time constants (mean ± SEM) are reported. **,***: *t* test $P < 0.01$ and $P < 0.001$ between LF and MF/HF neurons, respectively.

54.8 ± 10.3 ms, $n = 21$, $P < 0.001$, Fig. 1*H* and *I*; Table 1). The differences in the kinetics of sIPSCs and IPSCs between LF and MF/HF neurons were also manifested in the half-width of the IPSCs (Fig. 1*E* and *I*). The rise time of IPSCs of MF/HF neurons was also longer than that of LF neurons (LF: 1.6 ± 0.2 ms, $n = 21$; MF/HF: 2.9 ± 0.6 ms, $n = 21$, $P < 0.05$). For both LF and MF/HF neurons, the kinetics of evoked IPSCs was much slower than that of sIPSCs (Fig. 1*J*).

IPSC decay of MF/HF neurons is more strongly dependent on stimulus frequency and intensity than that of LF neurons

The GABAergic neurons in the SON projecting to the lower auditory brainstem nuclei including the NL fire at high discharge rates, with a spontaneous firing rate of about 30 Hz, and up to about 200 Hz when sound stimuli are present (Lachica *et al.* 1994; Coleman *et al.* 2011). To examine the properties of IPSCs under different stimulation conditions, we evoked IPSCs with train stimulations at 1, 5, 10, 50, 100 and 200 Hz. The stimulus intensity was kept constant across different stimulus frequencies. In MF/HF neurons, both the decay time constant and amplitude of the last stimulus pulse-induced IPSC increased dramatically with increasing stimulus frequency (Fig. 2*A–C*). At stimulus frequency of 1 Hz, relatively small IPSCs were observed with individual IPSC peaks clearly distinguishable. When the stimulus frequency was increased to 5 Hz, IPSCs of MF/HF neurons began to summate and did not return to baseline between stimulus pulses. At 100 Hz, a frequency of physiological relevance (Lachica *et al.* 1994; Coleman *et al.* 2011), IPSCs almost completely merged, generating a stable current plateau. In contrast, IPSCs of LF neurons were relatively stable in their amplitudes with increasing stimulus frequency. The decay time of IPSCs increased moderately at stimulus frequencies of 50 Hz and above. At all stimulus frequencies tested, the decay of IPSCs was significantly slower in MF/HF neurons than in LF neurons (Fig. 2*B*; Table 1). It is worth noting that in response to train stimulations, IPSCs of NL neurons displayed a mix of synaptic facilitation and depression, and the form of such short-term plasticity varied depending on stimulus frequencies (Fig. 2*D* and *E*), similar to the properties of the GABAergic transmission in NM neurons (Lu & Trussell, 2000). Interestingly, a transient synaptic facilitation was reliably observed at the second stimulus pulse in MF/HF neurons at all but 1 Hz stimulations. However, strong synaptic depression was observed for IPSCs in response to stimulus pulses after the second pulse. To further characterize the profile of short-term plasticity of IPSCs in NL neurons and to examine whether the differences in such properties correlate to the IPSCs of distinct kinetics between LF and MF/HF neurons, we studied recovery of IPSCs from depression using pair-pulse/train paradigms. Pair-pulse stimulation revealed a mix of facilitation and depression in both LF and MF/HF neurons (data not shown). When the second pulse in the pair-pulse protocol was preceded by train stimulation (100 Hz, 20 pulses), LF neurons ($n = 5$) displayed slight facilitation, whereas MF/HF neurons ($n = 5$) displayed depression (Fig. 2*F* and *G*).

Because the IPSC kinetics can also be affected by the amplitude of the currents, we compared the amplitude and decay of IPSCs obtained at high and low stimulus intensities (see Methods). The input–output functions of both LF and MF/HF neurons showed graded responses with increasing stimulus intensities (Fig. 3*A* and *B*). In response to single-pulse stimulations, IPSC amplitudes of both LF ($n = 9$) and MF/HF ($n = 14$) neurons were significantly higher at high stimulus intensity (Fig. 3*C–F*). The decays of IPSCs in the LF neurons were similar at the two stimulus intensities, whereas in the MF/HF neurons the decays at high stimulus intensity were significantly slower. Similar results were obtained when train stimulations (100 Hz, 20 pulses) were used to elicit IPSCs (Fig. 3*G–J*; Table 1). The dependence of IPSC decay time on the stimulation strength in the MF/HF neurons

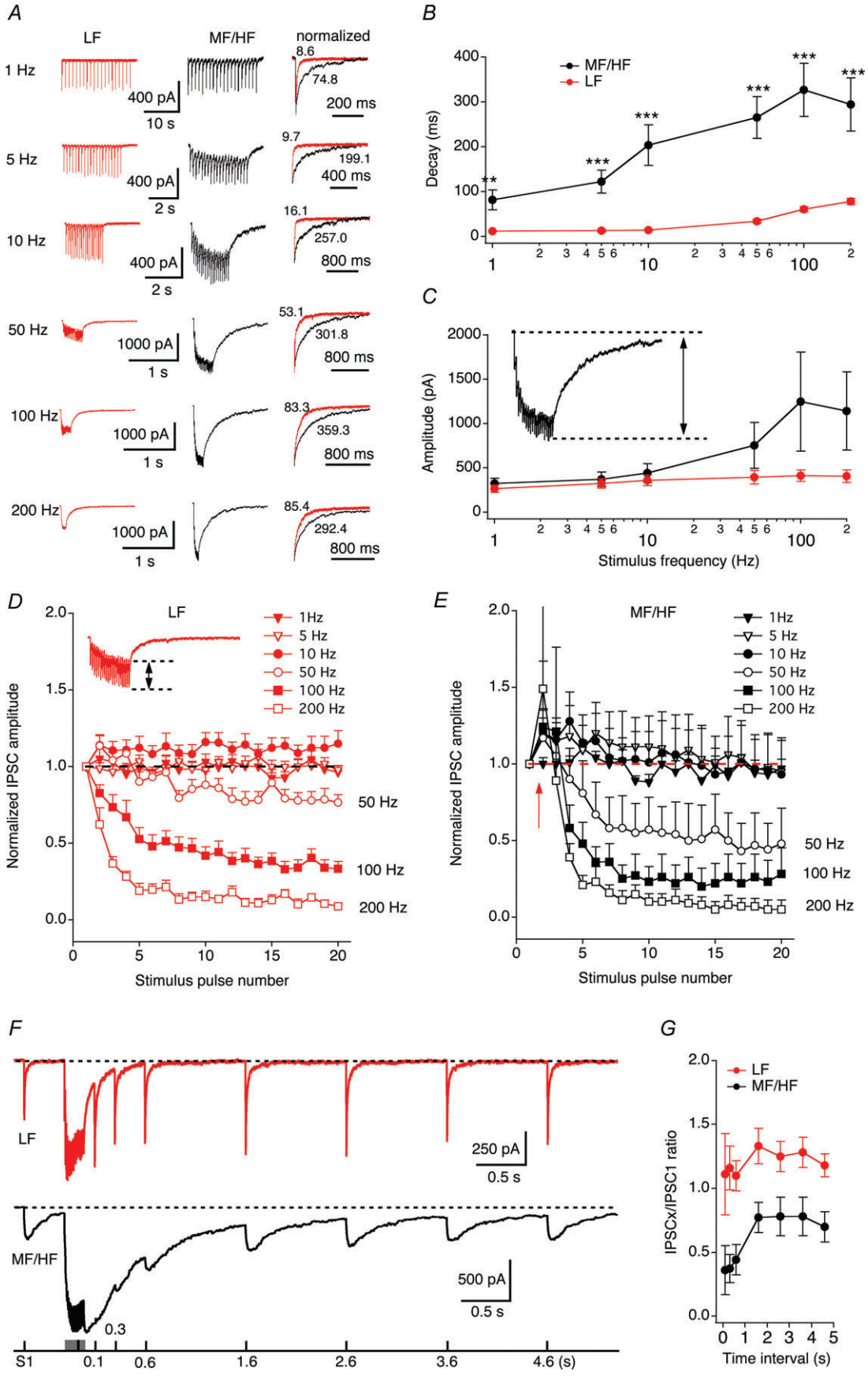

suggests that spillover of GABA onto nearby extrasynaptic $GABA_A$Rs might partly account for the slow IPSCs of these neurons. Stimulations at higher intensities would recruit more presynaptic fibres producing GABA pooling and slowing the decay of IPSCs (Rossi & Hamann, 1998; Balakrishnan *et al.* 2009).

It is well known that there exists a gradient of dendrite length along the tonotopic axis of the NL, i.e. LF neurons have long dendrites and HF neurons have short dendrites (Smith & Rubel, 1979). These morphological differences, however, are unlikely to interpret the kinetics differences in IPSCs between LF and MF/HF neurons. Dendritic filtering due to passive properties of neuronal membranes slows down the time course of postsynaptic currents recorded at the soma when the inputs sites are at distant dendrites (Rall, 1967), whereas voltage-gated conductances in dendrites may accelerate postsynaptic current kinetics (Mathews *et al.* 2010). Whether there are active conductances on the dendrites of NL neurons is as yet unknown. Because LF neurons have long dendrites and the GABAergic inputs are distributed along the entire dendrites (Carr *et al.* 1989; Code *et al.* 1989; Tabor *et al.* 2011), dendritic filtering would more extensively slow down IPSCs of LF neurons than MF/HF neurons, further increasing the differences in IPSC decay. Therefore, we hypothesized that other mechanisms accounted for the kinetics differences in IPSCs between LF and MF/HF neurons.

Asynchronous GABA release is more prominent in MF/HF neurons than in LF neurons

The fact that the decay of IPSCs strongly depends on stimulus frequency suggests that presynaptic asynchronous release (delayed release) of GABA may contribute to the slow GABAergic transmission in MF/HF neurons, as observed in other synapses (Lu & Trussell, 2000; Hefft & Jonas, 2005; Best & Regehr, 2009). We therefore examined the release events following the synchronized peak responses in IPSCs evoked by single-pulse stimulation (0.1 Hz) and train stimulation (100 Hz), which have been defined as asynchronous (delayed) release events (e.g. Atluri & Regehr, 1998; Lu & Trussell, 2000). In MF/HF neurons, such asynchronous quantal GABA releases were clearly observed for tens of milliseconds after the synchronized peak responses under both stimulus paradigms (Fig. 4). At the stimulus frequency of 0.1 Hz, the vast majority of IPSCs displayed a synchronous peak response followed by a considerable number of asynchronous release events. The frequency of asynchronous events counted in a 300 ms time window (onset at 50 ms after the onset of the stimulation) was much lower in LF neurons (5.7 ± 1.4 Hz, $n = 21$) compared to MF/HF neurons (23.4 ± 3.2 Hz, $n = 21$, $P < 0.001$) (Fig. 4*A* and *B*).

With train stimulations (100 Hz, 20 pulses), we observed an increase in the number of asynchronous releases that persisted for several seconds after the stimulation in both LF and MF/HF neurons (Fig. 4*C*–*F*). In MF/HF neurons, a massive increase (about 6-fold) in the frequency of asynchronous release was evident immediately after the termination of the train stimulation, with the frequency of asynchronous release detected in a 500 ms time window (onset at 300 ms after the onset of the train stimulation) being 50.2 ± 11.1 Hz ($n = 9$). In contrast, the frequency of asynchronous release in LF neurons was only 10.6 ± 1.3 Hz ($n = 13$, $P < 0.01$). Consistent with these observations, under minimal stimulation conditions (the smallest stimulus intensity at which synaptic responses were observed) LF neurons exhibited stimulus time-locked IPSCs, whereas in MF/HF neurons IPSCs were more scattered in timing of

Figure 2. IPSC decay of MF/HF neurons is more strongly dependent on stimulus frequency than that of LF neurons
A, average IPSCs in response to train stimulations at 1, 5, 10, 50, 100 and 200 Hz (20 pulses at each frequency). Shown on the right are superimposed last IPSCs normalized to the peak. The stimulus artifacts are blanked for clarity. The weighted decay time constants (ms) of individual traces are labelled. *B*–*C*, decay time constant and amplitude of the summed IPSCs elicited by the last stimulus pulse plotted against stimulus frequency (LF neurons, $n = 11$; MF/HF neurons, $n = 8$). The amplitude of the summed IPSCs was measured as the current difference between the baseline prior to the onset of the response and the peak of the last IPSC, as shown in the inset in panel *C*. Note the log scale for stimulus frequency. At all stimulus frequencies tested, the IPSC decays of MF/HF neurons were significantly slower than those of LF neurons. *D* and *E*, IPSC amplitude normalized to the first IPSC was plotted against the stimulus pulse number. The amplitude of each individual IPSC was measured as the current difference between the onset of the IPSC and its peak, as shown in the inset in panel *D*. Both LF and MF/HF neurons showed a mixed facilitation and depression in their IPSCs. The dashed lines indicate the baseline for normalization. The red arrow in *E* indicates the transient facilitation. *F* and *G*, short-term plasticity induced by train stimulation. Pair-pulse stimulation revealed a mix of facilitation and depression in both LF and MF/HF neurons (data not shown). When the second pulse in the pair-pulse protocol was preceded by train stimulation (100 Hz, 20 pulses), LF neurons ($n = 5$) displayed slight facilitation, whereas MF/HF neurons ($n = 5$) displayed depression. The time interval refers to the time difference between the second single pulse and the termination of the train stimulation.

their occurrence (Fig. 5*A*), consistent with the observation at the GABAergic synapses impinging upon the inferior olive from the deep cerebellar nuclei (Best & Regehr, 2009). Because synchrony of transmitter release increases over development (Chuhma & Ohmori, 1998; Chuhma *et al.* 2001), we further confirmed the observation of prominent asynchronous GABA release in MF/HF neurons in more mature animals (P3 chicks) (Fig. 5*B*;

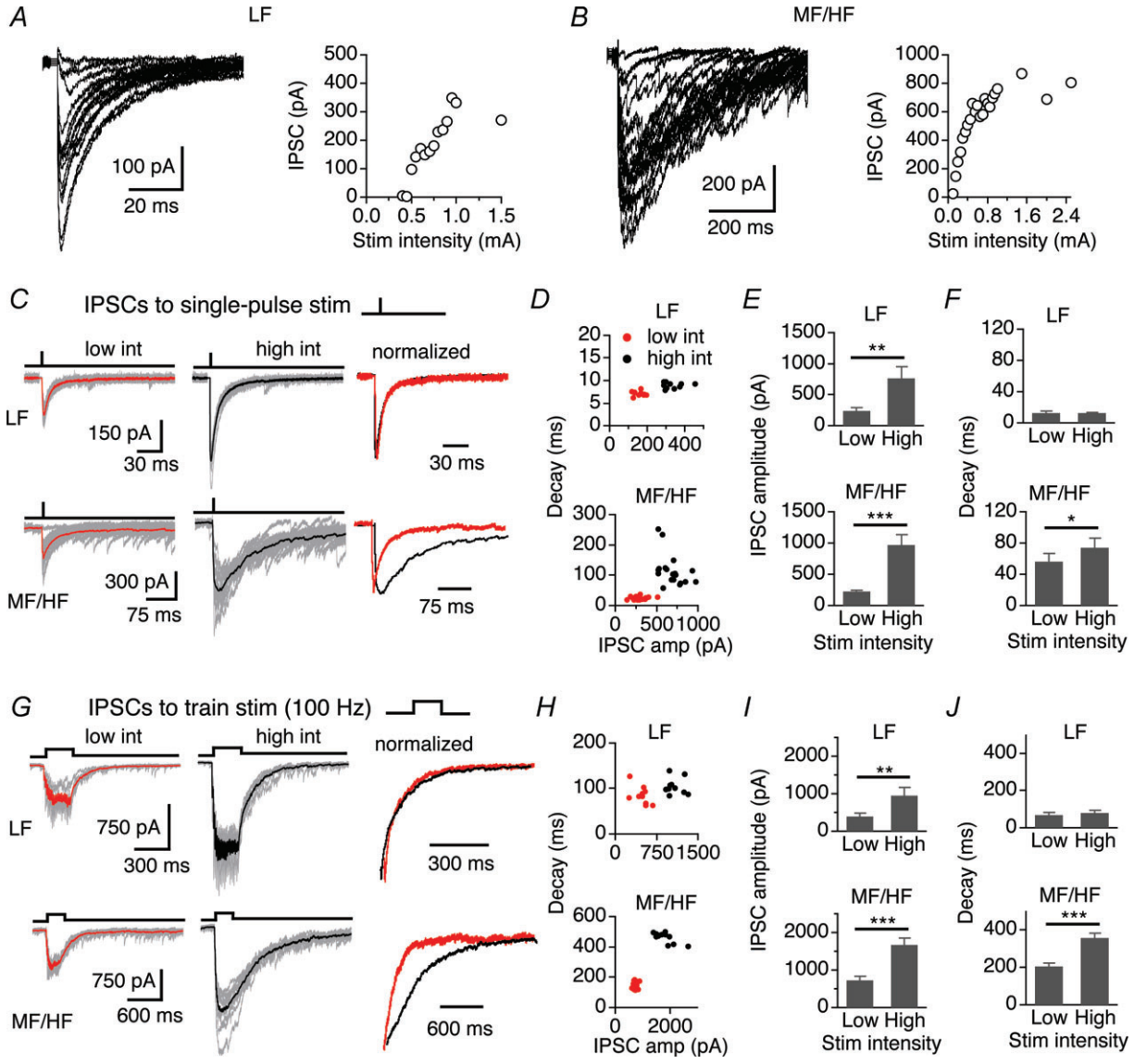

Figure 3. IPSC decay of MF/HF neurons is more strongly dependent on stimulus intensity than that of LF neurons

A and *B*, two representative recordings showing superimposed original IPSC traces at varying stimulus intensities. IPSC amplitudes increased with increasing stimulus intensities, resulting in graded input output functions in both LF and MF/HF neurons. *C*, superimposed individual IPSCs (grey) in response to single-pulse stimulations at two stimulus intensities with the average IPSCs highlighted (thick red and black traces). Right: average IPSCs normalized to the peak. *D*, distribution of the decays of individual IPSCs of the sampled neurons. *E*, in both LF ($n = 9$) and MF/HF ($n = 14$) neurons, the IPSC amplitude significantly increased with stimulus intensity. *F*, the IPSC decays in the LF neurons were similar at low and high stimulus intensities, whereas in the MF/HF neurons the decays at high stimulus intensity were significantly slower. *G*, superimposed individual IPSCs (grey) in response to train stimulations (100 Hz, 20 pulses) with the average IPSCs highlighted. Right, last IPSCs normalized to the peak. *H*, the distribution of decays of individual IPSCs of the sampled neurons. *I*, in both LF ($n = 7$) and MF/HF ($n = 15$) neurons the IPSC amplitude significantly increased with stimulus intensity. *J*, the decays of IPSCs in the LF neurons were similar at low and high stimulus intensities, whereas in the MF/HF neurons the decays at high stimulus intensity were significantly slower.

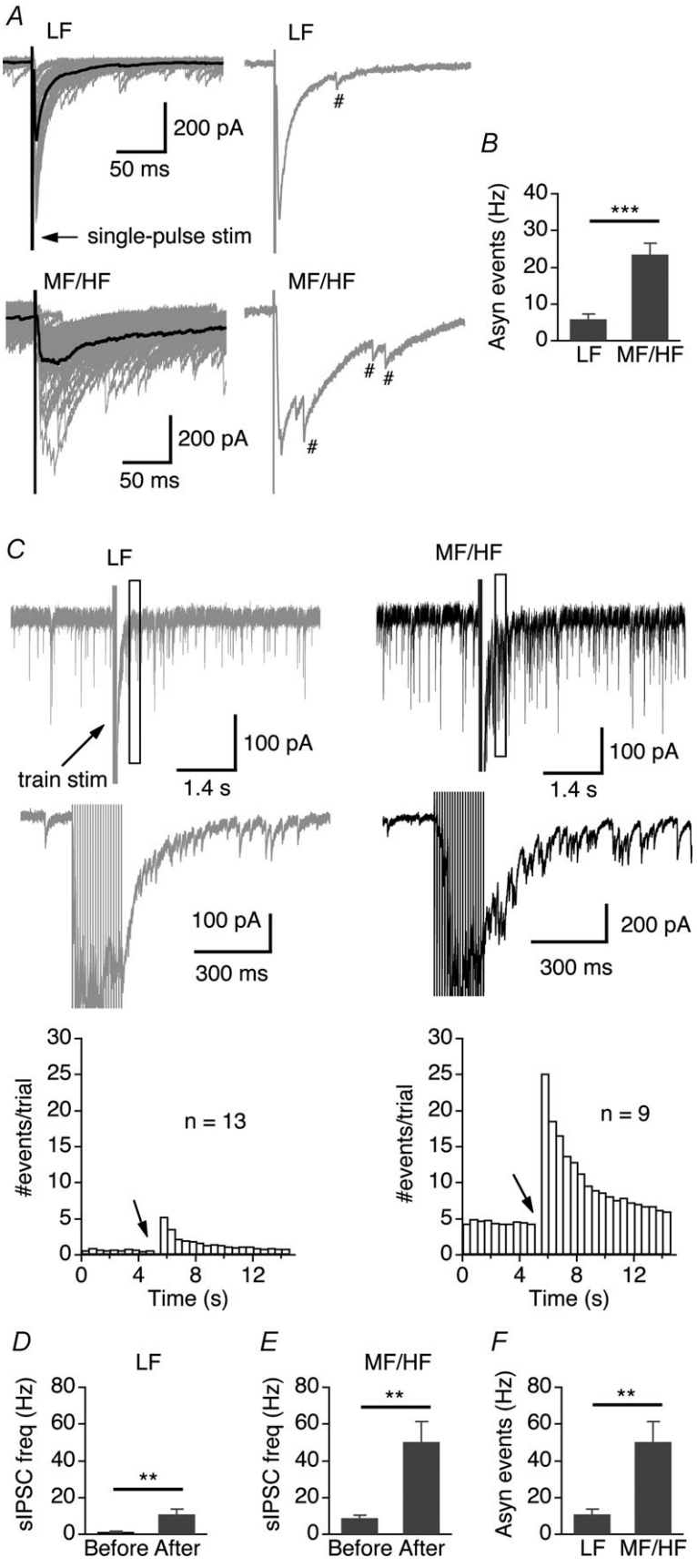

Figure 4. Asynchronous GABA release is more prominent in MF/HF neurons than in LF neurons
A, upper row, superimposed IPSCs (grey) elicited by single-pulse stimulation in a LF neuron with the average trace shown in black. Shown on the right is one individual IPSC with one asynchronous GABA release event labelled (#). Lower row, recordings from a MF/HF neuron. Multiple asynchronous release events were observed in response to the single stimulus. *B*, summary of frequency of asynchronous events counted in a 300 ms time window 50 ms after the stimulation (LF, $n = 21$; MF/HF, $n = 21$). *C*, upper row, single IPSCs elicited by a train stimulation (100 Hz, 20 pulses) from a LF neuron (grey) and a MF/HF neuron (black). The box indicates the time window (500 ms in duration, onset at 300 ms after the last stimulus pulse) within which asynchronous events were counted to make the graph in panel *F*. Middle row, part of the IPSCs shown at enlarged scales. Lower row, sIPSC event histograms plotted from 113 traces of 13 LF neurons and 82 traces of 9 MF/HF neurons (bin width: 0.5 s). Arrow indicates the onset of the train stimulation. We did not count sIPSCs within the first 0.3 s after the train stimulation because individual events could not be unambiguously detected during this period. *D–F*, although the sIPSC frequency significantly increased after the stimulation in both LF and MF/HF neurons, the asynchronous events in MF/HF neurons were significantly more frequent than in LF neurons, consistent with the observation under single-pulse stimulations.

LF: $n = 3$, MF/HF: $n = 4$). The decay time constants of IPSCs in these more mature NL neurons were much faster than those obtained from late embryos, and differed significantly between LF and MF/HF neurons (single-pulse stimulation, LF: 6.0 ± 1.1 ms, $n = 3$; MF/HF: 23.3 ± 5.6 ms, $n = 4$; $P < 0.05$; 100 Hz train stimulation, LF: 49.6 ± 12.9 ms, $n = 3$; MF/HF: 264.4 ± 33.5 ms, $n = 4$; $P < 0.01$).

To further confirm the differential profiles of asynchronous release of GABA in LF and MF/HF neurons, we examined the effects on IPSC decay of altered release patterns by manipulating cellular processes

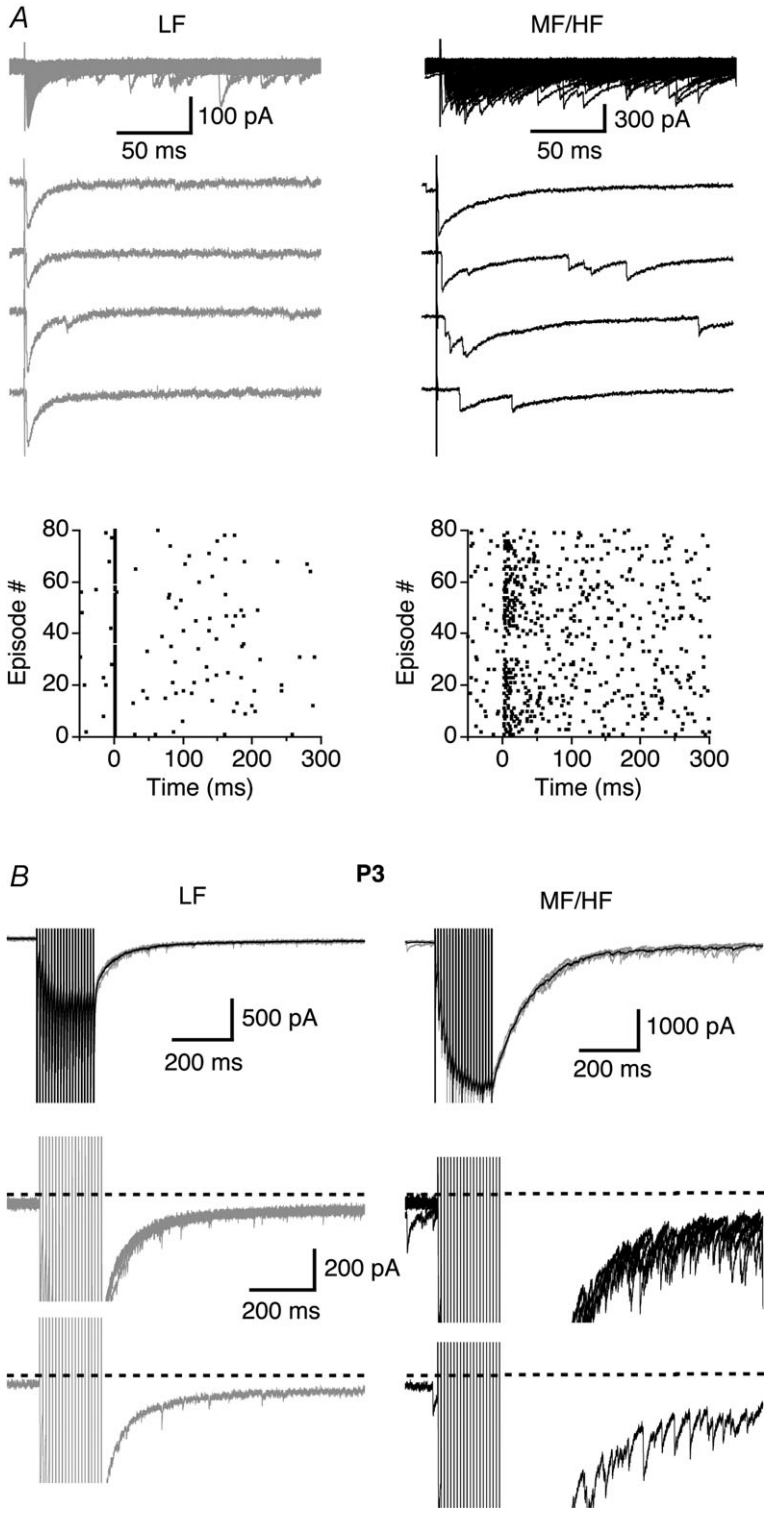

Figure 5. Prominent asynchronous GABA release was present in MF/HF neurons under minimal stimulation conditions and in more mature neurons
A, superimposed IPSCs (top) and four individual traces for each neuron elicited by single-pulse stimuli under minimal stimulation conditions. The LF neuron exhibited a stimulus time-locked response representing strong synchronous release, whereas in the MF/HF neuron IPSCs were more scattered in their timing of occurrence. The zero time point in the raster plots indicates the onset of the electrical stimulation. *B*, in P3 chicks, more prominent asynchronous release events seemed to be present in MF/HF neurons. Upper row, superimposed IPSCs (grey) elicited by train stimulations (100 Hz, 20 pulses) with the average trace shown in black. Middle and lower rows, superimposed IPSCs and one IPSC trace respectively from the upper row shown at an enlarged amplitude scale.

associated with Ca^{2+}. We replaced extracellular Ca^{2+} with 8 mM Sr^{2+}, a divalent cation that has been shown to induce asynchronous GABA release at inhibitory terminals (Morishita & Alger, 1997; Rumpel & Behrends, 1999), and compared the decay of IPSCs in the presence of Sr^{2+} with the control. As expected, Sr^{2+} enhanced asynchronous release and significantly increased the decay of IPSCs of LF neurons evoked by single or train stimuli (Fig. 6*A*–*D*). In MF/HF neurons, Sr^{2+} significantly prolonged the decay of IPSCs elicited with single-pulse stimulation, but did not affect IPSCs recorded with train stimulation (100 Hz, 20 pulses) (Fig. 6*E*–*H*, Table 2), suggesting that asynchronous release of GABA in MF/HF neurons might be at saturating levels under 100 Hz stimulation.

On the other hand, it is well known that asynchronous release results from a build-up of residual Ca^{2+} in the presynaptic terminals (Rahamimoff & Yaari, 1973; Goda & Stevens, 1994; Cummings *et al.* 1996; Atluri & Regehr, 1998; Lu & Trussell, 2000; Best & Regehr, 2009; Ali & Todorova, 2010) and can be controlled to a large extent by Ca^{2+} clearance (Goda & Stevens, 1994; Cummings *et al.* 1996). To confirm the involvement of residual Ca^{2+} in generating asynchronous release of GABA in NL neurons, we bath-applied (>5 min) a membrane-permeant Ca^{2+} chelator EGTA-AM while recording IPSCs, in order to buffer residual Ca^{2+} elevation and thereby reduce asynchronous release in presynaptic terminals (Atluri & Regehr, 1998; Lu & Trussell, 2000; Best & Regehr,

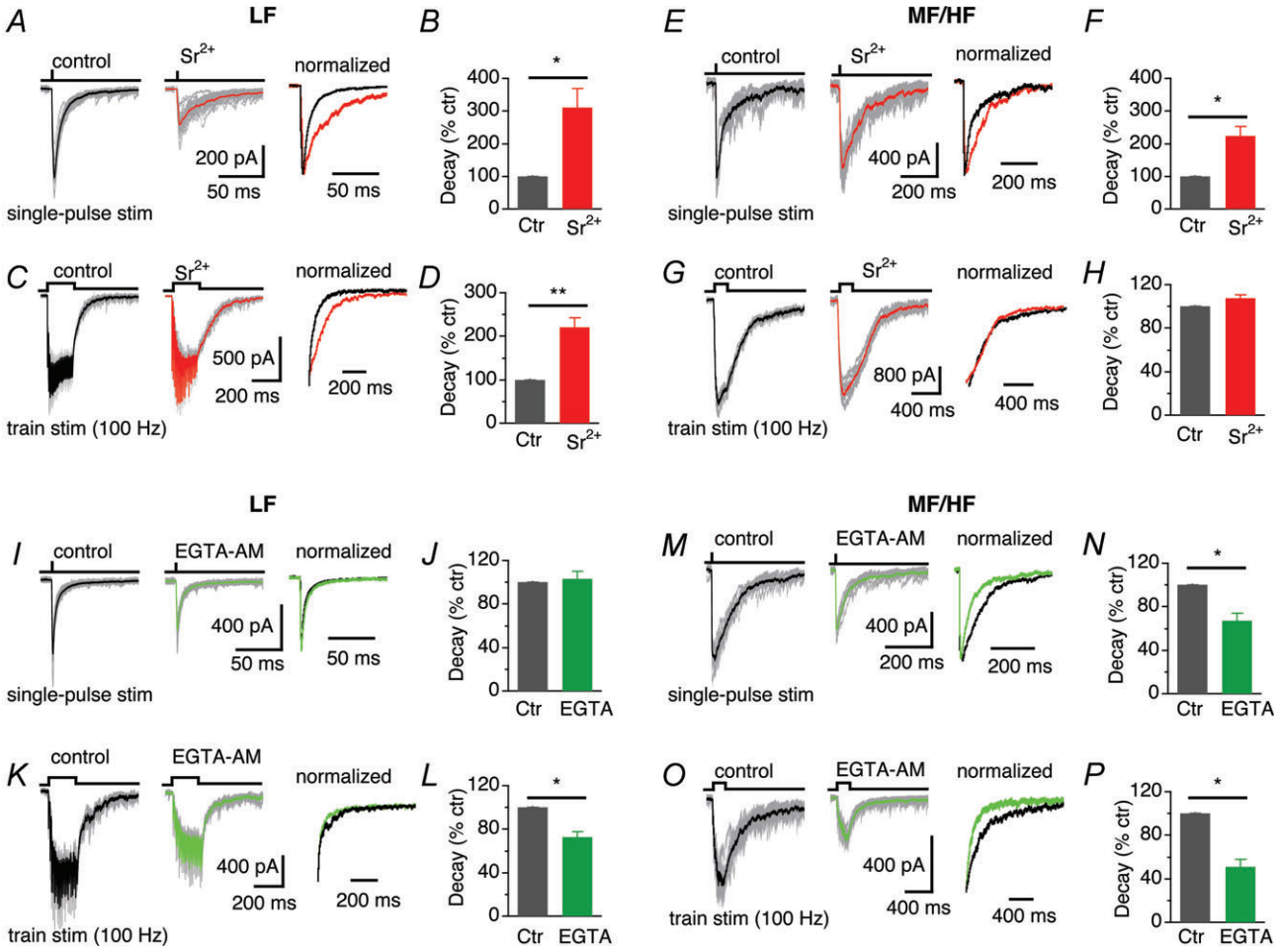

Figure 6. Manipulation of Ca^{2+} alters differently the decay of IPSCs in LF and MF/HF neurons
A, superimposed individual IPSCs (grey) of a LF neuron in response to single-pulse stimulation with the average IPSCs highlighted (thick traces), under the conditions of 3 mM Ca^{2+} (left) and in 8 mM Sr^{2+} (middle). Right, average IPSCs normalized to the peak. *B*, Sr^{2+} significantly prolonged the decay of IPSCs ($n = 5$). *C* and *D*, IPSCs of LF neurons in response to train stimulation (100 Hz, 20 pulses) were significantly prolonged by Sr^{2+} (8 mM) ($n = 6$). *E*–*H*, in MF/HF neurons, Sr^{2+} significantly prolonged IPSCs elicited with single-pulse stimulation ($n = 6$), but did not affect IPSCs recorded with train stimulation (100 Hz, 20 pulses) ($n = 6$). *I* and *J*, the decay of IPSCs of LF neurons in response to single-pulse stimulation was not affected by bath application (>5 min) of EGTA-AM (100 μM) ($n = 5$). *K* and *L*, in LF neurons, EGTA-AM accelerated the decay of IPSCs elicited with train stimulations (100 Hz, 20 pulses) ($n = 4$). *M*–*P*, EGTA-AM accelerated the decay of IPSCs in MF/HF neurons, regardless of the stimulus mode (single-pulse stimulation: $n = 7$, train stimulation: $n = 4$).

Table 2. Decay time constants (ms) of IPSCs of NL neurons under different drug and stimulus conditions

	LF			MF/HF		
Drug and stimulus	Control (*n*)	Drug	*P* value	Control (*n*)	Drug	*P* value
Sr^{2+}						
Single-pulse	10.6 ± 1.1(5)	32.6 ± 5.8	<0.05	50.6 ± 6.3(6)	103.5 ± 5.6	<0.05
100 Hz train	64.9 ± 5.7(6)	140.8 ± 16.2	<0.01	342.4 ± 36.2(6)	363.1 ± 31.9	>0.05
EGTA-AM						
Single-pulse	7.4 ± 1.0(5)	7.5 ± 0.9	>0.05	63.1 ± 20.2(7)	34.3 ± 8.5	<0.05
100 Hz train	67.4 ± 14.2(4)	46.8 ± 7.5	<0.05	305.0 ± 76.1(4)	120.8 ± 13.4	<0.05
NNC 771	69.3 ± 7.0(4)	70.0 ± 4.6	>0.05	250.5 ± 44.1(5)	290.1 ± 40.2	<0.05
TPMPA	44.0 ± 7.8(4)	34.3 ± 7.0	<0.05	334.6 ± 59.8(9)	233.0 ± 40.1	<0.001
SR95531	n.d.		n.d.	324.7 ± 42.9(6)	311.2 ± 50.7	>0.05
Low Ca^{2+}	80.7 ± 11.1(6)	46.2 ± 9.7	<0.05	264.6 ± 27.9(7)	174.0 ± 24.5	<0.001

n: number of cells; n.d.: not determined. Weighted time constants (mean ± SEM), and *P* values of paired *t* test are reported.

2009; Ali & Todorova, 2010). In LF neurons, EGTA-AM (100 μM) did not affect the decay of IPSCs elicited with single-pulse stimulation, but accelerated the decay of IPSCs recorded with train stimulations (100 Hz, 20 pulses) (Fig. 6*I–L*), suggesting the presence of a certain degree of asynchronous release of GABA under high but not low stimulus frequencies. In MF/HF neurons, EGTA-AM reduced the IPSC decay significantly regardless of the stimulus paradigms (Fig. 6*M–P*), confirming the presence of prominent asynchronous release of GABA in these neurons.

Spillover of GABA plays a greater role in prolonging IPSCs in MF/HF neurons than in LF neurons

The decay of IPSCs in MF/HF neurons of the NL (several hundred milliseconds under train stimulations) is much slower than that of IPSCs of neurons in other brain regions where prominent asynchronous GABA release was observed (Lu & Trussell, 2000; Hefft & Jonas, 2005; Best & Regehr, 2009). Therefore, we predicted that other mechanisms might exist to account for the unusually slow GABAergic transmission in MF/HF neurons. The observations that the decay time of IPSCs evoked by single-pulse stimulation in MF/HF neurons was much slower than that of sIPSCs (Fig. 1), and that the decay strongly depended on stimulus intensity (Fig. 3) suggest that GABA spillover may contribute to the slow IPSCs and the spillover may be more prominent in MF/HF neurons than in LF neurons. To test this hypothesis, we studied the effects on IPSC decays of blocking GABA transport, antagonizing $GABA_A$Rs with low-affinity antagonists, and lowering release probability.

One distinct feature of neurotransmitter spillover is that the postsynaptic currents are highly sensitive to the activity of neurotransmitter transporters (e.g. Balakrishnan *et al.* 2009; Thomas *et al.* 2011). To test whether GABA spillover contributed differentially to the decay of IPSCs between LF and MF/HF NL neurons, we examined the effects of a GABA transporter-1 (GAT-1) blocker NNC 711 on IPSCs elicited by 100 Hz train stimulation. Because GABA transporters rapidly take GABA back up into glial cells and/or presynaptic terminals, blockade of GABA transporters would prolong the presence of GABA in the synaptic cleft and surrounding areas, slowing the decay of IPSCs. Interestingly, in LF neurons, NNC 711 (10–20 μM) did not affect the decay of the IPSCs (Fig. 7*A* and *B*). In contrast, in MF/HF neurons, NNC 711 significantly prolonged the decay of the IPSCs (Fig. 7*C*, *D*). These results suggest that the GABA transporters in LF neurons are not the major players in shaping the fast kinetics of IPSCs. Additionally, NNC 711 reduced the amplitude of the IPSCs in both LF and MF/HF neurons, likely caused by desensitization of $GABA_A$Rs in the presence of prolonged GABA molecules after the uptake mechanisms were blocked (Rossi & Hamann, 1998; Overstreet *et al.* 2000). In addition, sIPSC decays of neither LF nor MF/HF neurons were altered by NNC 711 (LF, control, 6.8 ± 0.6 ms *versus* 6.8 ± 0.4, $n = 4$; MF/HF, control, 23.6 ± 0.9 ms *versus* 20.2 ± 2.3, $n = 4$), suggesting little modulation of sIPSC kinetics by GABA transporters. These data suggest that GABA spillover in MF/HF neurons is more prominent than in LF neurons.

Another distinct feature of neurotransmitter spillover is that the postsynaptic currents are particularly sensitive to low affinity competitive antagonists for postsynaptic receptors (Szabadics *et al.* 2007; Balakrishnan *et al.* 2009). Because they preferentially act on extrasynaptic receptors over synaptic receptors (Szabadics *et al.* 2007), low-affinity competitive antagonists for $GABA_A$Rs would accelerate the decay of the synaptic currents. To address this issue, we evaluated the effects of TPMPA, a weak, competitive antagonist for $GABA_A$Rs, on the IPSCs elicited by train stimulation at 100 Hz. Interestingly,

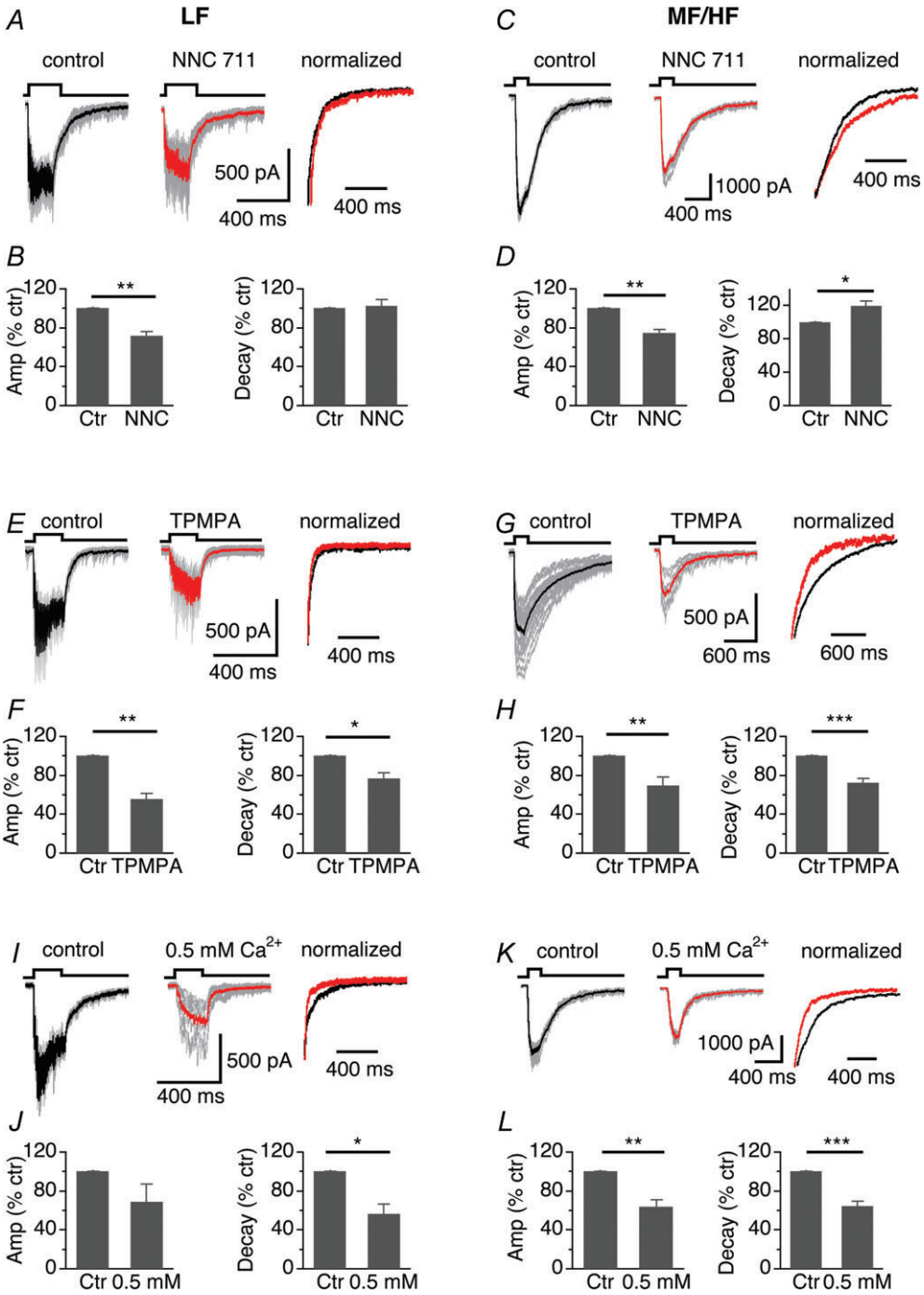

Figure 7. Spillover of GABA plays a greater role in prolonging IPSCs in MF/HF neurons than in LF neurons
A, IPSCs of a LF neuron in response to a train stimulation (100 Hz, 20 pulses) before and during application of NNC 711, a GABA transporter inhibitor. *B*, NNC 711 (10–20 μM) reduced the amplitude, without affecting the decay of IPSCs ($n = 4$). *C* and *D*, in MF/HF neurons, NNC 711 (10–20 μM) reduced the amplitude and prolonged the decay of IPSCs ($n = 5$), suggesting more prominent spillover of GABA in MF/HF neurons. *E–H*, in both LF and MF/HF neurons, a low affinity antagonist for $GABA_A$Rs, TPMPA (200 μM), significantly reduced the amplitude and decay of IPSCs (LF: $n = 4$; MF/HF: $n = 9$), suggesting the presence of extrasynaptic $GABA_A$Rs in both groups of cells. *I*, IPSCs of a LF neuron in response to a train stimulation (100 Hz, 20 pulses) under normal (3 mM) and reduced Ca^{2+} (0.5 mM) concentrations in ACSF. *J*, reducing Ca^{2+} in ACSF significantly reduced the decay, without affecting the amplitude of IPSCs ($n = 6$). *K* and *L*, in MF/HF neurons, reducing Ca^{2+} in ACSF significantly reduced the amplitude and decay of IPSCs ($n = 7$).

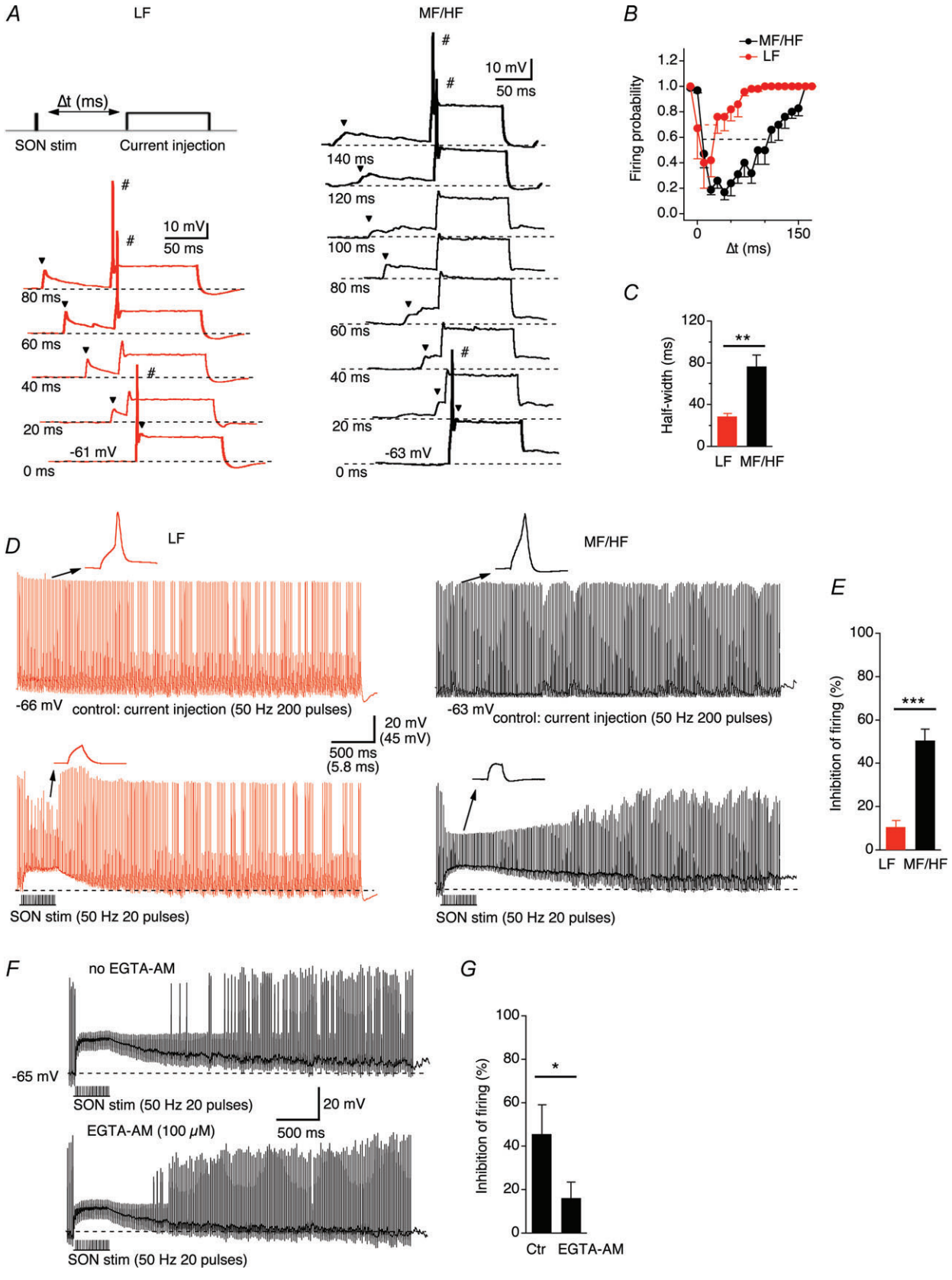

TPMPA (200 μM) application significantly reduced the amplitude and the decay of IPSCs in both LF and MF/HF neurons (Fig. 7*E–H*; Table 2), suggesting the presence of extrasynaptic $GABA_A$Rs in both groups of cells. This is consistent with the findings of our previous study (Tang *et al.* 2011), in which we demonstrated a tonic current mediated by extrasynaptic $GABA_A$Rs containing the δ subunit in NL neurons. In contrast, a high-affinity antagonist for $GABA_A$Rs (SR95531, at a sub-maximal concentration of 50 nM) caused a significant decrease in the amplitude of IPSCs (control, 1727.2 ± 275.2 pA *versus* SR95531, 1061.2 ± 204.2 pA, $n = 6$, $P < 0.001$), without changing the decay (Table 2). The lack of effects of SR95531 on the time course of IPSCs is possibly because the antagonist equally blocked the synaptic and extrasynaptic $GABA_A$Rs.

Finally, extrasynaptic low GABA concentration resulting from GABA spillover is expected to be affected by release probability. If GABA spillover contributed to the slow IPSC kinetics in MF/HF neurons, reducing synaptic release probability by lowering extracellular Ca^{2+} concentrations would reduce the decay time of IPSCs. To test this idea, we compared the IPSCs evoked by train stimulation at 100 Hz under conditions of low (0.5 mM) and normal (3 mM) extracellular Ca^{2+} concentrations. In LF neurons, low Ca^{2+} concentrations reduced the decay, without affecting the amplitude of IPSCs (Fig. 7*I* and *J*). In MF/HF neurons, under the conditions of low Ca^{2+} concentrations, the decay became faster, and the amplitude of IPSCs was significantly reduced (Fig. 7*K* and *L*; Table 2). Because lower Ca^{2+} concentrations led to faster IPSCs by reducing asynchronous release (Fig. 6), these results were likely the outcome of the combined effects of reduced asynchronous release as well as reduced spillover. Taken together, the effects on IPSC decays of NNC 711, TPMPA, and lower Ca^{2+} concentration suggest that GABA spillover in MF/HF neurons contributes more to the decay of IPSCs than in LF neurons.

The $GABA_A$R-mediated inhibition differentially regulates the neuronal excitability of LF and MF/HF neurons

Previous studies have shown that via a shunting effect, activation of K^+ channels and partial inactivation of Na^+ channels (Monsivais & Rubel, 2001; Tang *et al.* 2011), a depolarizing GABAergic inhibitioncan reduce the size and shorten the duration of EPSPs and may facilitate the coincidence detection in the NL neurons (Funabiki *et al.* 1998; Yang *et al.* 1999). Here, we further investigated the effects of synaptically released GABA on the excitability of NL neurons, and predicted that the GABAergic inhibition produced longer-lasting suppression of neuronal excitability in MH/HF than in LF neurons. We first altered the timing of the IPSP elicited by a single-pulse stimulus, and examined its effects on the spiking activity in response to a prolonged suprathreshold (100 pA above the current thresholds) somatic current injection. The single IPSP suppressed the firing, and the inhibition window (the width at 50% reduction in firing probability) was much longer in MF/HF neurons than in LF neurons (Fig. 8*A–C*, LF: 28.7 ± 3.1 ms, $n = 6$, MF/HF: 76.4 ± 11.1 ms, $n = 7$, $P < 0.01$). We then studied the effects of temporally summated IPSPs on NL excitability. Constant spiking activity was elicited by suprathreshold (100 pA above the current thresholds measured under the 50 Hz stimulus condition) somatic current injections (50 Hz, 200 pulses). Activation of the inhibitory pathway (SON stim, 50 Hz, 20 pulses) produced a prolonged inhibition that extended beyond the duration of the stimulation (Fig. 8*D*), consistent with previous studies (Yang *et al.* 1999). Interestingly, the inhibition in MF/HF neurons lasted longer and suppressed more spikes than in LF neurons (% inhibition of firing probability, LF: 10.7 ± 2.9, $n = 5$, MF/HF: 50.5 ± 5.2, $n = 7$, $P < 0.001$; Fig. 8*E*), apparently because the IPSP decayed more rapidly in LF neurons than in MF/HF neurons. To further correlate the GABA release profile to their firing properties, we took advantage of a previous finding that EGTA-AM treatment reduced

Figure 8. The $GABA_A$R-mediated inhibition differentially regulates the neuronal excitability of LF and MF/HF neurons
A, a single IPSP (indicated by the arrowhead) suppressed the firing of NL neurons in response to prolonged somatic current injections within a certain time window. The amplitude of the current injection was 100 pA above the current threshold (the minimum current needed to elicit action potentials) for a given recorded neuron. The time interval (Δt) is defined as the difference between the onset of the synaptic stimulation and the onset of the prolonged current pulse. The onsets of the traces are staggered for clarity, and the thick traces indicate suprathreshold responses. *B* and *C*, the half-width of the time window for inhibition (defined as the width at 50% reduction in firing probability) in LF neurons ($n = 6$) was significantly shorter than that in MF/HF neurons ($n = 7$). *D* and *E*, constant spiking activity was elicited by suprathreshold (100 pA above the current threshold) somatic current injections (50 Hz, 200 pulses). Activation of the inhibitory pathway (SON stim, 50 Hz, 20 pulses) produced temporally summated IPSPs of comparable amplitudes between LF and MF/HF neurons. However, a stronger inhibition of spiking activity was observed in MF/HF ($n = 7$) than LF neurons ($n = 5$). *F* and *G*, the SON stimulation-evoked inhibition of spiking activity in MF/HF neurons was significantly reduced by application of 100 μM EGTA-AM for $\geq$15 min ($n = 5$). The dashed lines in *A*, *D* and *F* indicate resting membrane potentials.

IPSC decay. If EGTA reduced IPSC decay by reducing asynchronous release of GABA, the effects on firing of SON stimulation in the presence of EGTA in MF/HF neurons would produce shorter inhibition duration. These predictions were indeed confirmed. Application of EGTA-AM (100 μM) for $\geq$15 min significantly reduced the SON stimulation-evoked inhibition of firing activity (% inhibition of firing probability, control: 45.5 $\pm$ 13.5; EGTA-AM: 16.0 $\pm$ 7.3, $n = 5$, $P < 0.05$; Fig. 8*F* and *G*).

Discussion

Our data clearly show that the kinetics of $GABA_A$R-mediated synaptic inhibition differs markedly between LF and MF/HF neurons. The differences are more substantial when the inhibitory inputs are driven by stimuli at frequencies relevant to the firing rates of the presynaptic GABA neurons. The morphological differences between LF and MF/HF neurons cannot be used to interpret these observations. Rather, our results indicate that differential profiles in asynchronous release along the tonotopic axis of the NL are the underlying mechanisms.

Asynchronous GABA release is more prominent in MF/HF than LF neurons

Previous studies have shown that asynchronous release of neurotransmitters can significantly affect the kinetics of IPSCs (Lu & Trussell, 2000; Best & Regehr, 2009; Ali & Todorova, 2010) and EPSCs (Diamond & Jahr, 1995; Iremonger & Bains, 2007). In the NL, considerable asynchronous GABA release occurred in MF/HF neurons in response to both single-pulse and train stimulations. Following train stimulations at physiologically relevant frequencies (100 Hz), many asynchronous release events persisted for several seconds in MF/HF neurons. In contrast, asynchronous release was hardly detectable in LF neurons with single-pulse stimulus, and fewer asynchronous release events were observed at high frequency stimulations.

Differences in a number of factors could account for the differential asynchronous release profiles between LF and MF/HF neurons. First, the sources of the GABAergic inputs may be different. Asynchronous release is dependent on the class of presynaptic neurons and independent of postsynaptic cell type (Daw *et al.* 2009), so two scenarios may be speculated: (1) different populations of SON cells project to different CF regions of NL, and (2) local GABA cells project to LF region while SON projections mainly target MF/HF neurons. Recently Tabor *et al.* (2011) reported that the projections from the SON to NL are coarsely tonotopic. It is possible that the GABAergic cells of the SON that innervate the MF/HF neurons of the NL may have differential release properties from those that innervate the LF neurons.

Second, potential differences in presynaptic Ca^{2+} signalling triggering GABA release should be considered. Presynaptic N-type voltage-gated Ca^{2+} channels (VGCCs) are more closely associated with asynchronous release than P/Q-type VGCCs in hippocampal neurons (Hefft & Jonas, 2005). Given that N-type channels trigger GABA release in NL neurons regardless of CF regions (Lu, 2009), the types of presynaptic VGCCs cannot account for the differences in IPSC kinetics between LF and MF/HF neurons. However, the properties of the molecular events linking the Ca^{2+} entry via presynaptic VGCCs to exocytosis of synaptic vesicles might dramatically differ. For example, differences in the distance coupling Ca^{2+} entry and the Ca^{2+} sensor (Rozov *et al.* 2001), the duration of Ca^{2+} transients in the presynaptic terminals (Atluri & Regehr, 1998), and the affinity of the Ca^{2+} sensor in the presynaptic terminals (Hui *et al.* 2005) can lead to dramatically different profiles in asynchronous release. Differential modulation of GABA release by other receptor systems such as the cannabinoid receptors could also produce different asynchronous release profiles (Ali & Todorova, 2010). One very recent study reveals that the expression level of a SNARE protein VAMP4 defines the extent of asynchronous neurotransmission (Raingo *et al.* 2012). Future studies need to determine whether such mechanisms account for the difference in GABA release pattern between LF and MF/HF NL neurons.

GABA spillover plays a greater role in prolonging IPSCs in MF/HF neurons than in LF neurons

In this study, several lines of evidence suggest that GABA spillover plays a greater role in prolonging IPSCs in MF/HF neurons. First, the kinetics of IPSCs in MF/HF neurons displayed stronger dependency on stimulus frequency and intensity than LF neurons. The progressive increase in the decay time of IPSCs was closely associated with an increase in stimulus frequency, consistent with observations at the synapses between deep cerebellar nuclei and the inferior olive where asynchronous release of GABA is prominent at stimulus frequencies of 10 Hz and above (Best & Regehr, 2009). The strong dependency of the IPSC decay on stimulus intensity also suggests that GABA spillover onto nearby synapses and/or extrasynaptic $GABA_A$Rs might contribute to the slow IPSCs in MF/HF neurons. Stimulations at higher intensity would recruit more fibres producing GABA pooling and slowing the decay of IPSCs (Rossi & Hamann, 1998; Balakrishnan *et al.* 2009). Second, pharmacological evidence indicates that GABA spillover contributes to form the slow IPSCs in NL neurons. The spillover transmitter-mediated currents have characteristic features, such as their high sensitivity to blockade of GABA transporters, to low-affinity

competitive antagonists, and to alterations in release probability (Szabadics *et al.* 2007). Indeed, blocking GABA uptake prolonged the IPSC decays in MF/HF but not LF neurons. However, the decay of IPSCs was accelerated by TPMPA as well as by reduced extracellular Ca^{2+} in both LF and MF/HF neurons, pointing to the possibility that GABA spillover might contribute to the decay of the IPSCs in both groups of cells. The precise proportional contribution of asynchronous release *versus* spillover of GABA to the decay of IPSCs was not examined because of the lack of feasible approaches to distinguish these two processes.

Finally, we consider other possible factors. Postsynaptic receptors could differ in their subunit composition and hence different affinity and time course of IPSCs (Banks *et al.* 1998). Developmental changes in subunit composition (Tia *et al.* 1996), and desensitization properties of $GABA_A$Rs are also contributors to GABA responses with changing kinetics (Karayannis *et al.* 2010). The most likely interpretation for the significant difference in the decay of sIPSCs between LF and MF/HF neurons may be different subunit composition. Because the majority sIPSCs of NL neurons recorded in our slice preparations presumably represented miniature IPSCs caused by single vesicle release, it is conceivable that neither asynchronous release nor spillover of GABA, phenomena of multiple vesicle release, would form a feasible explanation for the differential decays of sIPSCs between LF and MF/HF neurons. Rather, changes in subunit content, binding affinity and gating mechanisms of $GABA_A$Rs may account for the differences. Taken together, mechanisms involving both presynaptic GABA release and postsynaptic receptor subtypes may contribute to form distinct $GABA_A$ responses in different CF regions of the NL.

Functional implication

The differences in release patterns may define functional division of NL neurons in the ITD encoding process. Previous studies have shown that GABAergic inhibition evoked by direct stimulation of the SON reduces the amplitude of EPSP and inhibits spike firing in NL neurons (Yang *et al.* 1999), and exogenous GABA application facilitates the coincidence detection of the bilateral excitatory inputs to the NL neurons (Brückner & Hyson, 1998; Funabiki *et al.* 1998). Our present study extends these studies by assessing the effects of synaptically released GABA on the excitability of NL neurons in different CF regions. On one hand, consistent with Yang *et al.* (1999), we found that synaptically released GABA in response to train stimulations generated temporally summated depolarizing IPSPs in both LF and MF/HF neurons. Such sustained inhibition would result in a leaky membrane and render the membrane's fast response to strong converging excitatory inputs, improving the precision of the coincidence detection of the bilateral excitatory inputs. The implication of sustained inhibition of different durations in different CF neurons is unclear, and this is one limitation of our current study. We speculate that the longer-lasting inhibition in MF/HF neurons may improve the extent of segregation of the two excitatory inputs onto the same NL neuron, enhancing the effectiveness of synaptic integration of the bilateral inputs. Previous computer modelling studies have assumed a complete segregation of the two excitatory inputs to the coincidence detectors (e.g. Agmon-Snir *et al.* 1998), but experimental evidence is absent. Our unpublished data suggested that the degree of segregation was incomplete (about 80% in MF/HF neurons), and our future studies will systematically assess the extent of segregation along the tonotopic axis of the NL. We hypothesize that without the regulation of synaptic inhibition, the degree of segregation of the bilateral excitatory inputs in MF/HF neurons may be less complete than in LF neurons. It remains to be determined how synaptic inhibitions with distinct kinetics properties affect such parameters in NL neurons. On the other hand, IPSP elicited by single-pulse stimulation produced a short time window in LF neurons during which the excitability was suppressed. Such fast IPSPs would play a more transient modulatory role in the ITD coding than the slow IPSPs would in MF/HF neurons, if the firing rates of the presynaptic GABA neurons innervating the LF neurons were low. Given the heterogeneity of SON neurons (Carr *et al.* 1989; Lachica *et al.* 1994) and the strong phase-locking capabilities of some SON neurons (Coleman *et al.* 2011), more transient GABA inputs in LF neurons may exist, providing phasic inhibition to modulate ongoing highly phase-locked excitatory inputs. Taken together, these results suggest that the GABAergic inputs to NL neurons may exert a dynamic modulation of ITD coding in a CF-dependent manner.

References

Agmon-Snir H, Carr CE & Rinzel J (1998). The role of dendrites in auditory coincidence detection. *Nature* **393**, 268–272.

Ali AB & Todorova M (2010). Asynchronous release of GABA via tonic cannabinoid receptor activation at identified interneuron synapses in rat CA1. *Eur J Neurosci* **31**, 1196–1207.

Atluri PP & Regehr WG (1998). Delayed release of neurotransmitter from cerebellar granule cells. *J Neurosci* **18**, 8214–8227.

Banks MI, Li TB & Pearce RA (1998). The synaptic basis of $GABA_{A,slow}$. *J Neurosci* **18**, 1305–1317.

Balakrishnan V, Kuo SP, Roberts PD & Trussell LO (2009). Slow glycinergic transmission mediated by transmitter pooling. *Nat Neurosci* **12**, 286–294.

Best AR & Regehr WG (2009). Inhibitory regulation of electrically coupled neurons in the inferior olive is mediated by asynchronous release of GABA. *Neuron* **62**, 555–565.

Brückner S & Hyson RL (1998). Effect of GABA on the processing of interaural time differences in nucleus laminaris neurons in the chick. *Eur J Neurosci* **10**, 3438–3450.

Burger RM, Cramer KS, Pfeiffer JD & Rubel EW (2005). Avian superior olivary nucleus provides divergent inhibitory input to parallel auditory pathways. *J Comp Neurol* **481**, 6–18.

Burger RM, Fukui I, Ohmori H & Rubel EW (2011). Inhibition in the balance: binaurally coupled inhibitory feedback in sound localization circuitry. *J Neurophysiol* **106**, 4–14.

Capogna M & Pearce RA (2011). $GABA_{A,slow}$: causes and consequences. *Trends Neurosci* **34**, 101–112.

Carr CE, Fujita I & Konishi M (1989). Distribution of GABAergic neurons and terminals in auditory system of the barn owl. *J Comp Neurol* **286**, 190–207.

Chuhma N & Ohmori H (1998). Postnatal development of phase-locked high-fidelity synaptic transmission in the medial nucleus of the trapezoid body of the rat. *J Neurosci* **18**, 512–520.

Chuhma N, Koyano K & Ohmori H (2001). Synchronisation of neurotransmitter release during postnatal development in a calyceal presynaptic terminal of rat. *J Physiol* **530**, 93–104.

Code RA, Burd GD & Rubel EW (1989). Development of GABA immunoreactivity in brainstem auditory nuclei of the chick: ontogeny of gradients in terminal staining. *J Comp Neurol* **284**, 504–518.

Coleman WL, Fischl MJ, Weimann SR & Burger RM (2011). GABAergic and glycinergic inhibition modulate monaural auditory response properties in the avian superior olivary nucleus. *J Neurophysiol* **105**, 2405–2420.

Cummings DD, Wilcox KS & Dichter MA (1996). Calcium-dependent paired-pulse facilitation of miniature EPSC frequency accompanies depression of EPSCs at hippocampal synapses in culture. *J Neurosci* **16**, 5312–5323.

Farrant M & Nusser Z (2005). Variations on an inhibitory theme: phasic and tonic activation of $GABA_A$ receptors. *Nat Rev Neurosci* **6**, 215–229.

Funabiki K, Koyano K & Ohmori H (1998). The role of GABAergic inputs for coincidence detection in the neurones of nucleus laminaris of the chick. *J Physiol* **508**, 851–869.

Daw MI, Tricoire L, Erdelyi F, Szabo G & McBain CJ (2009). Asynchronous transmitter release from cholecystokinin-containing inhibitory interneurons is widespread and target-cell independent. *J Neurosci* **29**, 11112–11122.

Diamond JS & Jahr CE (1995). Asynchronous release of synaptic vesicles determines the time course of the AMPA receptor-mediated EPSC. *Neuron* **15**, 1097–1107.

Goda Y & Stevens CF (1994). Two components of transmitter release at a central synapse. *Proc Natl Acad Sci U S A* **91**, 12942–12946.

Grothe B (2003). New roles for synaptic inhibition in sound localization. *Nat Rev Neurosci* **4**, 540–550.

Hefft S & Jonas P (2005). Asynchronous GABA release generates long-lasting inhibition at a hippocampal interneuron-principal neuron synapse. *Nat Neurosci* **8**, 1319–1328.

Hui E, Bai J, Wang P, Sugimori M, Llinas RR & Chapman ER (2005). Three distinct kinetic groupings of the synaptotagmin family: candidate sensors for rapid and delayed exocytosis. *Proc Natl Acad Sci U S A* **102**, 5210–5214.

Iremonger KJ & Bains JS (2007). Integration of asynchronously released quanta prolongs the postsynaptic spike window. *J Neurosci* **27**, 6684–6691.

Kandler K, Clause A & Noh J (2009). Tonotopic reorganization of developing auditory brainstem circuits. *Nat Neurosci* **12**, 711–717.

Karayannis T, Elfant D, Huerta-Ocampo I, TeKi S, Scott RS, Rusakov DA, Jones MV & Capogna M (2010). Slow GABA transient and receptor desensitization shape synaptic responses evoked by hippocampal neurogliaform cells. *J Neurosci* **30**, 9898–9909.

Köppl C & Carr CE (2008). Maps of interaural time difference in the chicken's brainstem nucleus laminaris. *Biol Cybern* **98**, 541–559.

Kuba H, Yamada R, Fukui I & Ohmori H (2005). Tonotopic specialization of auditory coincidence detection in nucleus laminaris of the chick. *J Neurosci* **25**, 1924–1934.

Kuba H, Ishii TM & Ohmori H (2006). Axonal site of spike initiation enhances auditory coincidence detection. *Nature* **444**, 1069–1072.

Kuo SP, Bradley LA & Trussell LO (2009). Heterogeneous kinetics and pharmacology of synaptic inhibition in the chick auditory brainstem. *J Neurosci* **29**, 9625–9634.

Lachica EA, Rübsamen R & Rubel EW (1994). GABAergic terminals in nucleus magnocellularis and laminaris originate from the superior olivary nucleus. *J Comp Neurol* **348**, 403–418.

Lu T & Trussell LO (2000). Inhibitory transmission mediated by asynchronous transmitter release. *Neuron* **26**, 683–694.

Lu Y (2009). Regulation of glutamatergic and GABAergic neurotransmission in the chick nucleus laminaris: role of N-type calcium channels. *Neuroscience* **164**, 1009–1019.

Mathews PJ, Jercog PE, Rinzel J, Scott LL & Golding NL (2010). Control of submillisecond synaptic timing in binaural coincidence detectors by K_v1 channels. *Nat Neurosci* **13**, 601–609.

Monsivais P & Rubel EW (2001). Accommodation enhances depolarizing inhibition in central neurons. *J Neurosci* **21**, 7823–7830.

Morishita W & Alger BE (1997). Sr^{2+} supports depolarization-induced suppression of inhibition and provides new evidence for a presynaptic expression mechanism in rat hippocampal slices. *J Physiol* **505**, 307–317.

Nishino E, Yamada R, Kuba H, Hioki H, Furuta T, Kaneko T & Ohmori H (2008). Sound-intensity-dependent compensation for the small interaural time difference cue for sound source localization. *J Neurosci* **28**, 7153–7164.

Overstreet LS, Jones MV & Westbrook GL (2000). Slow desensitization regulates the availability of synaptic $GABA_A$ receptors. *J Neurosci* **20**, 7914–7921.

Pearce RA (1993). Physiological evidence for two distinct $GABA_A$ responses in rat hippocampus. *Neuron* **10**, 189–200.

Rahamimoff R & Yaari Y (1973). Delayed release of transmitter at the frog neuromuscular junction. *J Physiol* 228, 241–257.

Raingo J, Khvotchev M, Liu P, Darios F, Li YC, Ramirez DM, Adachi M, Lemieux P, Toth K, Davletov B & Kavalali ET (2012). VAMP4 directs synaptic vesicles to a pool that selectively maintains asynchronous neurotransmission. *Nat Neurosci* **15**, 738–745.

Rall W (1967). Distinguishing theoretical synaptic potentials computed for different soma-dendritic distributions of synaptic input. *J Neurophysiol* **30**, 1138–1168.

Rossi DJ & Hamann M (1998). Spillover-mediated transmission at inhibitory synapses promoted by high affinity α6 subunit $GABA_A$ receptors and glomerular geometry. *Neuron* **20**, 783–795.

Rozov A, Burnashev N, Sakmann B & Neher E (2001). Transmitter release modulation by intracellular Ca^{2+} buffers in facilitating and depressing nerve terminals of pyramidal cells in layer 2/3 of the rat neocortex indicates a target cell-specific difference in presynaptic calcium dynamics. *J Physiol* **531**, 807–826.

Rubel EW & Parks TN (1975). Organization and development of brain stem auditory nuclei of the chicken: tonotopic organization of n. magnocellularis and n. laminaris. *J Comp Neurol* **164**, 411–433.

Rumpel E & Behrends JC (1999). Sr^{2+}-dependent asynchronous evoked transmission at rat striatal inhibitory synapses *in vitro*. *J Physiol* **514**, 447–458.

Sanchez JT, Wang Y, Rubel EW & Barria A (2010). Development of glutamatergic synaptic transmission in binaural auditory neurons. *J Neurophysiol* **104**, 1774–1789.

Seidl AH, Rubel EW & Harris DM (2010). Mechanisms for adjusting interaural time differences to achieve binaural coincidence detection. *J Neurosci* **30**, 70–80.

Slee SJ, Higgs MH, Fairhall AL & Spain WJ (2010). Tonotopic tuning in a sound localization circuit. *J Neurophysiol* **103**, 2857–2875.

Smith DJ & Rubel EW (1979). Organization and development of brain stem auditory nuclei of the chicken: dendritic gradients in nucleus laminaris. *J Comp Neurol* **186**, 213–239.

Szabadics J, Tamás G & Soltesz I (2007). Different transmitter transients underlie presynaptic cell type specificity of $GABA_{A,slow}$ and $GABA_{A,fast}$. *Proc Natl Acad Sci U S A* **104**, 14831–14836.

Tabor KM, Wong RO & Rubel EW (2011). Topography and morphology of the inhibitory projection from superior olivary nucleus to nucleus laminaris in chickens (*Gallus gallus*). *J Comp Neurol* **519**, 358–375.

Tang ZQ, Gao H & Lu Y (2009). Control of a depolarizing GABAergic input in an auditory coincidence detection circuit. *J Neurophysiol* **102**, 1672–1683.

Tang ZQ, Dinh EH, Shi W & Lu Y (2011). Ambient GABA-activated tonic inhibition sharpens auditory coincidence detection via a depolarizing shunting mechanism. *J Neurosci* **31**, 6121–6131.

Tia S, Wang JF, Kotchabhakdi N & Vicini S (1996). Developmental changes of inhibitory synaptic currents in cerebellar granule neurons: role of $GABA_A$ receptor α6 subunit. *J Neurosci* **16**, 3630–3640.

Thomas CG, Tian H & Diamond JS (2011). The relative roles of diffusion and uptake in clearing synaptically released glutamate change during early postnatal development. *J Neurosci* **31**, 4743–4754.

Yamada R, Kuba H, Ishii TM & Ohmori H (2005). Hyperpolarization-activated cyclic nucleotide-gated cation channels regulate auditory coincidence detection in nucleus laminaris of the chick. *J Neurosci* **25**, 8867–8877.

Yang L, Monsivais P & Rubel EW (1999). The superior olivary nucleus and its influence on nucleus laminaris: a source of inhibitory feedback for coincidence detection in the avian auditory brainstem. *J Neurosci* **19**, 2313–2325.

Author contributions

Z.T. and Y.L. designed the study. Z.T. performed the experiments and analysed the data. Z.T. and Y.L. interpreted the data, and drafted and revised the article.

Acknowledgements

We thank Drs Joshua Gittelman, MacKenzie Howard and Jason Sanchez for critical comments on an earlier version of the manuscript. This work was supported by National Institute on Deafness and Other Communication Disorders Grant R01 DC008984 to Y.L.